



1

2

3

4

5

6

7

8

9

10

11

12

13

14

15

16

17

18

19

20

21

22

23

24

25

26

27

28

## High Enrichment of Heavy Metals in Fine Particulate Matter through Dust Aerosol Generation

**Authors:** Qianqian Gao<sup>1,2#</sup>, Shengqiang Zhu<sup>1#</sup>, Kaili Zhou<sup>1,2</sup>, Jinghao Zhai<sup>3</sup>,  
Shaodong Chen<sup>1,2</sup>, Qihuang Wang<sup>1,2</sup>, Shurong Wang<sup>1</sup>, Jin Han<sup>1,2</sup>, Xiaohui Lu<sup>1,2</sup>,  
Hong Chen<sup>1</sup>, Liwu Zhang<sup>1,2</sup>, Lin Wang<sup>1,2</sup>, Zimeng Wang<sup>1,2</sup>, Xin Yang<sup>3</sup>, Qi Ying<sup>4</sup>,  
Hongliang Zhang<sup>\*1</sup>, Jianmin Chen<sup>1,2\*</sup> and Xiaofei Wang<sup>\*1,2</sup>

<sup>1</sup>Shanghai Key Laboratory of Atmospheric Particle Pollution and Prevention,  
Department of Environmental Science and Engineering, Fudan University, Shanghai  
200433, China

<sup>2</sup>Shanghai Institute of Pollution Control and Ecological Security, Shanghai  
200092, China

<sup>3</sup>School of Environmental Science and Engineering, Southern University of  
Science and Technology, Shenzhen 518055, China

<sup>4</sup>Zachry Department of Civil Engineering, Texas A&M University, College  
Station, TX 77843, USA

#These authors contributed equally to this paper

\*To whom correspondence should be addressed.

Correspondence to:

Xiaofei Wang: Email: [xiaofeiwang@fudan.edu.cn](mailto:xiaofeiwang@fudan.edu.cn) Tel: +86-021-31242526

Jianmin Chen: Email: [jmchen@fudan.edu.cn](mailto:jmchen@fudan.edu.cn) Tel: +86(021)3124-2298

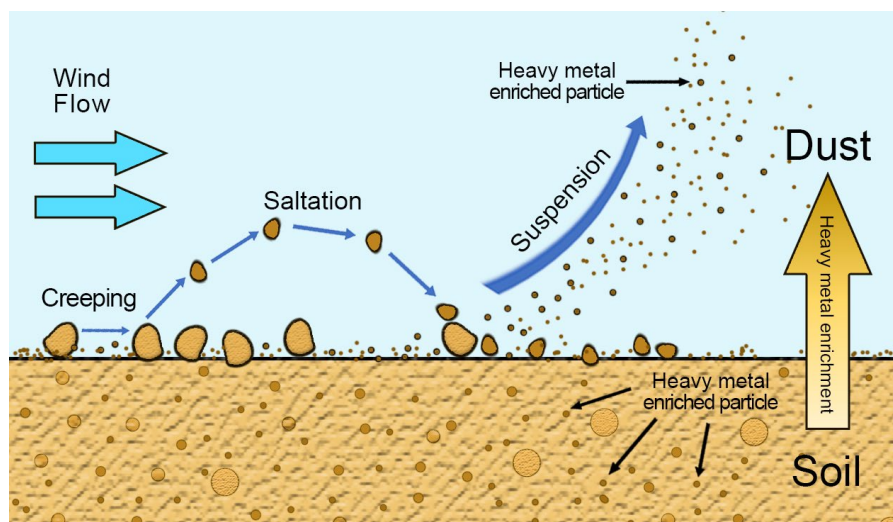
Hongliang Zhang: Email: [zhanghl@fudan.edu.cn](mailto:zhanghl@fudan.edu.cn) Tel: +86-021-31248978



## 29 Abstract

30 Dust is a major source of atmospheric aerosols. Its chemical composition is often assumed to be  
31 similar to the parent soil. However, this assumption has not been rigorously verified. Here, we  
32 generated dust aerosols from soils to determine if there is particle size-dependent selectivity of  
33 heavy metals in the dust generation. Mn, Cd, Pb and other heavy metals were found to be highly  
34 enriched in fine ( $PM_{2.5}$ ) dust aerosols, which can be up to ~6.5-fold. To calculate the contributions  
35 of dust to atmospheric heavy metals, regional air quality models usually use the dust chemical  
36 profiles from the US EPA's SPECIATE database, which does not capture the correct size-dependent  
37 selectivity of heavy metals in dust aerosols. Our air quality modeling for China demonstrates that  
38 the calculated contribution of fine dust aerosols to atmospheric heavy metals, as well as their cancer  
39 risks, could have significant errors without using proper dust profiles.

## 40 Graphical Abstract



41  
42



43 **Short Summary**

44 Dust is a major source of atmospheric aerosols. Its chemical composition is often assumed to be  
45 similar to the parent soil. However, this assumption has not been rigorously verified. Dust aerosols  
46 are mainly generated by wind erosion, which may have some chemical selectivity. Mn, Cd and Pb  
47 were found to be highly enriched in fine ( $PM_{2.5}$ ) dust aerosols. In addition, estimation of heavy  
48 metal emission from dust generation by air quality models may have errors without using proper  
49 dust profiles.

50



## 51 **1 Introduction**

52 The major sources of natural aerosols include mineral dust aerosols produced by wind erosion  
53 (Prospero et al., 2002). Dust aerosols are influenced by regional atmospheric circulation, soil  
54 characteristics and local weather conditions (Bryant, 2013; Ding et al., 2005; Huebert et al., 2003;  
55 Liu et al., 2004; Yang et al., 2008), mainly generated and aerosolized when strong wind passes over  
56 soil or sandy areas (Gillette and Goodwin, 1974). Recent studies show mineral dust aerosol accounts  
57 for approximately 40% of the mass fraction of natural atmospheric aerosol, with an estimated annual  
58 flux of  $\sim 2,000 \text{ Tg}\cdot\text{yr}^{-1}$  (Alfaro, 2008; Griggs and Noguera, 2002; Huneeus et al., 2011; Textor et al.,  
59 2006). As the second-largest natural source of atmospheric aerosols in terms of mass flux, dust  
60 aerosol has a profound impact on the ecosystem (Middleton et al., 2019), especially the climate  
61 (Evan et al., 2014; Kok et al., 2018; Shao et al., 2013). Interactions between dust aerosols and water  
62 vapor play a critical role in cloud condensation and ice nucleation processes (Kaufman et al., 2002;  
63 Tang et al., 2016). Dust particles can be transported on large scales (Shao and Dong, 2006), and  
64 could act as a medium to transport toxic compounds, including heavy metals, which significantly  
65 harm human health, particularly the human respiratory system and even cause premature death  
66 (Urrutia-Pereira et al., 2021).

67 Atmospheric studies often assume that the chemical composition of aerosolized dust is similar to  
68 the parent soil (Gunawardana et al., 2012; Zhuang et al., 2001). The chemical composition of dust  
69 aerosol consists of a key part in source apportionment modeling (Balakrishna and Pervez, 2009;  
70 Samiksha et al., 2017; Santos et al., 2017; Ying et al., 2018). A critical approach in source  
71 apportionment modeling is the chemical transport model, which predicts the dust aerosol on global



72 and regional scales based on the prior knowledge of source emission, atmospheric transport, and  
73 chemical reaction process. SPECIATE is the EPA's speciation profiles repository of air pollution  
74 sources of volatile organic compounds (VOCs) and particulate matter (PM). Therefore, the US  
75 EPA's SPECIATE database is an important product to convert total emissions from specific sources  
76 into the speciated emissions needed for the chemical transport model. The previous study has  
77 combined the US EPA's SPECIATE database and air quality model to predict dust aerosols (Ying et  
78 al., 2018), based on the assumption of the chemical composition of dust aerosols is similar to the  
79 resuspended soil profiles.

80 Yet, dust generation and aerosolization are complex processes, which may have some chemical  
81 selectivity. Most small dust particles ( $< 20 \mu\text{m}$ ) are produced either by wind erosion, which leads to  
82 soil movements such as creeping, saltation, and suspension (Burezq, 2020) or sandblasting process,  
83 which leads soil particles ( $\sim 75 \mu\text{m}$ ) to be lifted by the wind, move in ballistic trajectories due to the  
84 combined effect of aerodynamic force and gravity force (Grini and Zender, 2004; Shao and Raupach,  
85 1993; Shao et al., 1996). The sandblasting efficiency of a soil particle is highly sensitive to its size  
86 (Grini and Zender, 2004; Grini et al., 2002). In addition, the chemical composition of soil particles  
87 can also vary with particle size. As smaller soil particles are more easily ejected, dust aerosol  
88 particles are unlikely to have exactly the same composition as their parent soils (Perlwitz et al., 2015;  
89 Wu et al., 2022). Dust deposited samples were the dust samples collected on the road or other  
90 surfaces using a brush and plastic tray (Shangguan et al., 2022), while dust aerosol samples were  
91 collected by filtering the air. Dust aerosols were produced by the ballistic impacts of wind-driven  
92 sand grains (Kok et al., 2023). Indeed, some previous studies do find that in the deposited dust  
93 samples (not dust aerosol samples), smaller particles tend to contain higher amounts of heavy metals



94 (Naderizadeh et al., 2016; Parajuli et al., 2016; Becagli et al., 2020). However, the heavy metal  
95 profiles for dust aerosols from the US EPA's SPECIATE database seem to have no such enrichment  
96 between each particle size, as Table S1 reports profile 41350 as an example. Although these profiles  
97 have been widely used in air quality modeling works (Lowenthal et al., 2010; Simon et al., 2010;  
98 Ashrafi et al., 2018), they were actually measured in the 1970s and 1980s with the resuspension of  
99 soil samples, which placed soil in a glass tube and drew air flow to blow and suspend the soil  
100 particles to the air (Miller et al., 1972). This method is not likely to produce realistic dust aerosols,  
101 as it does not simulate sandblasting process properly. It is not known whether using such a  
102 problematic dust profile could significantly impact air quality model calculations.

103

104 Here we examined the enrichment of heavy metals in the laboratory-generated dust aerosols. A dust  
105 aerosol generator that mimics realistic sandblasting and saltation was used to generate dust aerosol  
106 from a collection of soil samples (Lafon et al., 2014). The concentrations of heavy metals in soil  
107 and dust aerosols were measured by an inductively coupled plasma mass spectrometer (ICP-MS).  
108 In this study, some heavy metals, such as Mn, Cd, Zn and Pb, were found to be highly enriched in  
109 dust aerosols. Especially, the enrichment factors would be much higher for smaller dust aerosols. In  
110 addition, we also utilized a single particle aerosol mass spectrometer (SPAMS) to study heavy metal-  
111 containing dust aerosols before, during, and after a dust storm. Regional air quality models usually  
112 use problematic dust composition profiles from the US EPA's SPECIATE database. Herein we  
113 modeled the contribution of dust aerosol to atmospheric heavy metal loadings, utilizing a range of  
114 dust aerosol profiles determined in this laboratory study as well as the SPECIATE profile, to  
115 investigate whether using a proper dust profile is critical to air quality modeling and cancer risk



116 calculations.

## 117 **2 Materials and methods**

### 118 **2.1 Soil sample collection**

119 Fourteen samples were collected from the top 10 cm of the natural soil profile from various locations  
120 in dust source regions and Shanghai, China (Table S2, Fig. S1). S1-S4 were collected from dust  
121 sources on the northern slope of Yinshan Mountain in central inner Mongolia and the adjacent areas  
122 of the Hunshandake Sandy Land, S5-S12 were collected from dust sources of Hexi Corridor and  
123 Alxa Plateau, S13 was collected in Xinjiang Province, in the dust sources of the Taklimakan Desert,  
124 and S14 was sampled from Shanghai Yangpu District. As shown in Table S2, they represent several  
125 soil types: S1 was silty loam; S2, S4, S7, S10, S11 and S12 were sand; S3 was sandy loam; S5 and  
126 S6 were loam; S8 and S13 were loam sand; S9 and S14 were silty clay loam. Before dust aerosol  
127 generation, soil samples were placed in a fume hood and left to dry, without stirring or other  
128 treatment, before aerosolization. Fine and coarse dust aerosols (PM<sub>2.5</sub> and PM<sub>10</sub>) were produced  
129 with a GAMEL dust aerosol generator, which can realistically simulate the sandblasting process.  
130 Then, the pH of the soil was measured. Detailed information can be found in Fig. S1 and Table S2.

### 131 **2.2 Laboratory dust aerosol generation and collection**

132 A laboratory dust generator (GAMEL: “Générateur d’Aérosol Minéral En Laboratoire”) (Lafon et  
133 al., 2014) was used to produce dust aerosols from the soil samples. The GAMEL dust generator can  
134 realistically simulate the sandblasting process. In GAMEL’s dust production system, 10 g of each  
135 soil sample was added to a PTFE flask, which was agitated by a shaker simulating the sandblasting



136 process to produce dust aerosols. A constant flow of particle-free air was passed through the dust-  
137 generating flask. The optimal generation parameter of the shaker was set at a frequency of 500  
138 cycles/min according to Lafon et al., 2014 with an airflow rate of 8 liter/min controlled by a Mass  
139 Flow Controller (MFC, Sevenstar, Beijing Sevenstar Flow Co., LTD). The sample stream was  
140 filtered through a cyclone and particles were collected on a 47 mm PVC film held in a metal frame  
141 filter holder (Pall Gelman, Port Washington, NY, USA). Dust-PM<sub>2.5</sub> and dust-PM<sub>10</sub> were obtained  
142 with or without an 8LPM cyclone, respectively. The running time was 1min. To obtain more dust  
143 aerosols in different size ranges, size-fractionated particle sampling of dust aerosols was carried out  
144 with 10-stage Micro-Orifice Uniform Deposit Impactor (MOUDI 110R; MSP) with size cut points  
145 of 10 μm, 5.6 μm, 3.2 μm, 1.8 μm, 1.0 μm, and 0.56 μm. Analysis of the size distribution and  
146 chemical composition of dust generated by GAMEL and dust generated under natural conditions  
147 has shown that the GAMEL generator can produce realistic dust aerosol (Lafon et al., 2014). All  
148 the dust aerosol mass collected is shown in Table S3 and S4. The instrument setup is illustrated  
149 in Fig. S2.

150

### 151 **2.3 Analysis of laboratory-generated dust aerosols**

152 The dust aerosol samples collected were weighed with an analytical balance and then put into 25 ml  
153 digestion tubes with 6 ml 69 % HNO<sub>3</sub> symmetrically. The temperature program of Microwave  
154 Digestion (Anton Paar) was as follows: initial temperature of 100 °C held for 5 min, then ramped  
155 to 140 °C for 5 min, and finally at 180 °C for 60 min. The whole process was holding 120 min.  
156 According to this study (Chang et al., 1984), almost all the heavy metal elements in the natural soil





157 and dust aerosol in concentrated nitric acid were extracted using this experimental procedure. After  
158 digestion, the solution was acid-fed at 120 °C for 1.5 h, then deionized water (conductivity 18.25  
159 MΩ) was added, the volume was constant with a 25 mL volumetric flask, and then passed through  
160 a 0.45 μm membrane. The samples were diluted with 2 % HNO<sub>3</sub> by 4 times for further analysis.  
161 Three blank PVC film samples were digested using the same method for background control.

162

163 The heavy metal content was determined by inductively coupled plasma mass spectrometer (ICP-  
164 MS; Agilent, 8900). Before analysis, tuning procedures including plasma parameter, ion  
165 transmission path, quadrupole mass spectrometer, and detector had been done. During analysis,  
166 standard solutions were prepared at concentrations of 0, 1, 2, 5, 10, 20, 50, and 100 μg/L. "In, Bi,  
167 and Rn" were used as internal standard elements, and were introduced into the nebulizer by mixing  
168 with the sample to be tested and the standard solution in the sampling pipeline by online addition,  
169 and the instrument drift and matrix effect were compensated. After each analysis of a sample, 2 %  
170 dilute nitric acid was used to clean the injection line for 1 min, and then continue to collect the  
171 second sample to eliminate the memory effect of the previous sample.

172 A scanning electron microscope (SEM; Phenom Pro) equipped with an energy-dispersive X-ray  
173 detector was used for morphologies of particle examination at the voltage of 10 kV. All the samples  
174 (soil, PM<sub>2.5</sub> and PM<sub>10</sub>) were on the carbon conductive adhesive, then spray platinum to improve the  
175 conductivity. Here, the parent soil of S10 and generated PM<sub>2.5</sub> and PM<sub>10</sub> were examined.

176 Statistical analysis was performed using SPSS Statistics. The correlation analysis was conducted  
177 through Spearman's correlation and the significant difference was used with an independent sample  
178 T-test.



179 **2.4 Ambient dust aerosol measurements**

180 On-site field measurements of ambient dust particles were conducted in Shanghai on May 23<sup>rd</sup>, 2018  
181 (LT). The sampling was located on the sixth floor of the Environmental Science Building in  
182 Jiangwan Campus, Fudan University, a typical residential area in a heavily polluted urban area. The  
183 chemical composition of individual ambient particles was measured by single particle aerosol mass  
184 spectrometry (SPAMS, Hexin Co., Ltd). Detailed information on SPAMS is available elsewhere (Li  
185 et al., 2011). An adaptive resonance theory-based clustering method (ART-2a) was used to classify  
186 the mass spectra generated and identify dust/heavy-metal-containing particles (Sullivan et al., 2007).  
187 The Hybrid Single-Particle Lagrangian Integrated Trajectory HYSPLIT-4 model developed by the  
188 ARL (Air Resources Laboratory) of the NOAA (National Oceanic and Atmospheric Administration),  
189 USA, was employed to compute hourly resolved 48 h air mass backward trajectories at 500 m arrival  
190 height (Lv et al., 2021; Pongkiatkul and Kim Oanh, 2007).

191

192 **2.5 Air quality model configuration and application**

193 The source-oriented CMAQ model v5.0.1 with an expanded SAPRC-99 photochemical mechanism  
194 was applied to simulate PM<sub>2.5</sub> levels and track the sources of primary PM<sub>2.5</sub> (PPM<sub>2.5</sub>) in China during  
195 the entire year of 2013 (Guenther et al., 2012; Ying et al., 2018). The simulation domain covered  
196 China and its surrounding countries, with a horizontal resolution of 36 × 36 km<sup>2</sup> (127 × 197 grids).  
197 Anthropogenic emissions were based on the Multi-resolution Emission Inventory for China (MEIC,  
198 v1.3, 0.25° × 0.25°, <http://www.meicmodel.org>). Biogenic emissions were generated by the Model  
199 of Emissions of Gases and Aerosols from Nature (MEGAN) v2.1 (Guenther et al., 2012). The



200 meteorological inputs for the CMAQ model were calculated by the Weather Research and  
201 Forecasting (WRF) model (<https://www2.mmm.ucar.edu/wrf/users>).

202

203 Five major source contributions (windblown dust, residential, transportation, power generation and  
204 industrial sources) to PM<sub>2.5</sub> were investigated based on the inventory-observation-constrained  
205 emission factors (Ying et al., 2018). Three control trials were conducted for each heavy metal  
206 according to the minimum, average, and maximum enrichment factors for the dust aerosols  
207 generated from the soil collected from the four regions (three dust sources and Shanghai). A no-  
208 enrichment trial was also conducted for comparison. It is noticeable that the enrichment factors  
209 outside these four regions were estimated by inverse distance weight (IDW) spatial interpolation  
210 methods (Zhang and Tripathi, 2018). The ratio of each heavy metal source contribution from dust  
211 aerosol and all four sources were used to quantify the enrichment effect on heavy metal  
212 concentrations in the atmospheric dust aerosols, which can be represented in Equation 1:

$$213 \quad R = \frac{E_1 \times s_1 \times a}{\sum_{i=1}^5 E_i \times s_i} \quad \text{Equation 1}$$

214 Where  $E_i$  is the PPM<sub>2.5</sub> emission from  $i^{\text{th}}$  source,  $s_i$  is the emission factor of the specific heavy metal  
215 from  $i^{\text{th}}$  source,  $a$  is the enrichment factor of this heavy metal in dust-PM<sub>2.5</sub>.  $E_i$ ,  $s_i$ , and  $a$  are the  
216 values for dust.

217 In addition, the human health risk of heavy metals was assessed. Three main routes of chemical  
218 daily intake (CDI, mg kg<sup>-1</sup> day<sup>-1</sup>) of air heavy metals were: (1) direct ingestion of particles or gases  
219 existed in the air (CDI<sub>ing</sub>); (2) inhalation of suspended particles through mouth and nose (CDI<sub>inh</sub>);  
220 and (3) daily absorption of heavy metals through skin (CDI<sub>dermal</sub>) (Luo et al., 2012). Specifically,  
221 the carcinogenic and non-carcinogenic effects of heavy metals were assessed in the 13 age groups  
222 in detail (from birth to ≤ 80 years old). CDI<sub>ing</sub>, CDI<sub>inh</sub>, and CDI<sub>dermal</sub> were calculated as:

223



$$CDI_{ing} = C \times \frac{IR_{ing} \times EF \times ED}{BW \times AT} \times 10^{-6} \quad \text{Equation 2}$$

$$CDI_{dermal} = C \times \frac{SA \times AF \times ABS_d \times EF \times ED}{BW \times AT} \times 10^{-6} \quad \text{Equation 3}$$

$$CDI_{inh} = C \times \frac{IR_{inh} \times ET \times EF \times ED}{BW \times AT} \times 10^{-6} \quad \text{Equation 4}$$

Moreover, the total carcinogenic risk (TCR) for each heavy metal were calculated by:

$$\text{carcinogenic risk} = CDI_{ing,dermal,inh} \times CSF \quad \text{Equation 5}$$

$$TCR = \sum risk = CDI_{ing} \times CSF_{ing} + CDI_{inh} \times IUR +$$

$$CDI_{dermal} \times CSF_{ing}/ABS_{GI} \quad \text{Equation 6}$$

232

Here the  $IR_{ing}$  was Ingestion rate ( $\text{mg day}^{-1}$ ),  $EF$  was exposure frequency ( $\text{day year}^{-1}$ ),  $ED$  was exposure duration (year),  $BW$  was body weight (kg),  $AT$  was Averaging time (day),  $SA$  was total body skin surface area ( $\text{m}^2$ ),  $AF$  was skin adherence factor ( $\text{mg cm}^{-2}$ ),  $ET$  was exposure time ( $\text{hour day}^{-1}$ ),  $ABS_d$  was dermal absorption factor,  $IR_{inh}$  inhalation rate ( $\text{m}^3 \text{day}^{-1}$ ),  $ABS_{GI}$  was gastrointestinal absorption factor,  $CSF$  was cancer slope factor. The values of these parameters could be found in the previous study (Gholizadeh et al., 2019).

239

## 240 3 Results and discussion

### 241 3.1 Enrichment of heavy metals in fine dust aerosols

242

243 . Fig. S3-S4 show the absolute concentrations of heavy metals in dust aerosols and their parent soils.

244 The concentrations of heavy metals in dust- $PM_{10}$  were similar to soil concentrations, which showed  
245 a significant correlation between soils and  $PM_{10}$  ( $p < 0.01$ ) (Fig. S5). While the concentrations of  
246 heavy metals in dust- $PM_{2.5}$  were higher than those in soils, especially Mn, Ni, Cu and Zn, showed  
247 significant differences ( $p < 0.001$ ) (Fig. S6). This trend was consistent across all soil samples. The



248 enrichment factor (EF) of heavy metals in dust aerosols relative to the parent soils was calculated  
249 with Equation 8.

$$250 \quad EF = \frac{C_1/m_1}{C_0/m_0} \dots \dots \dots \text{Equation 8}$$

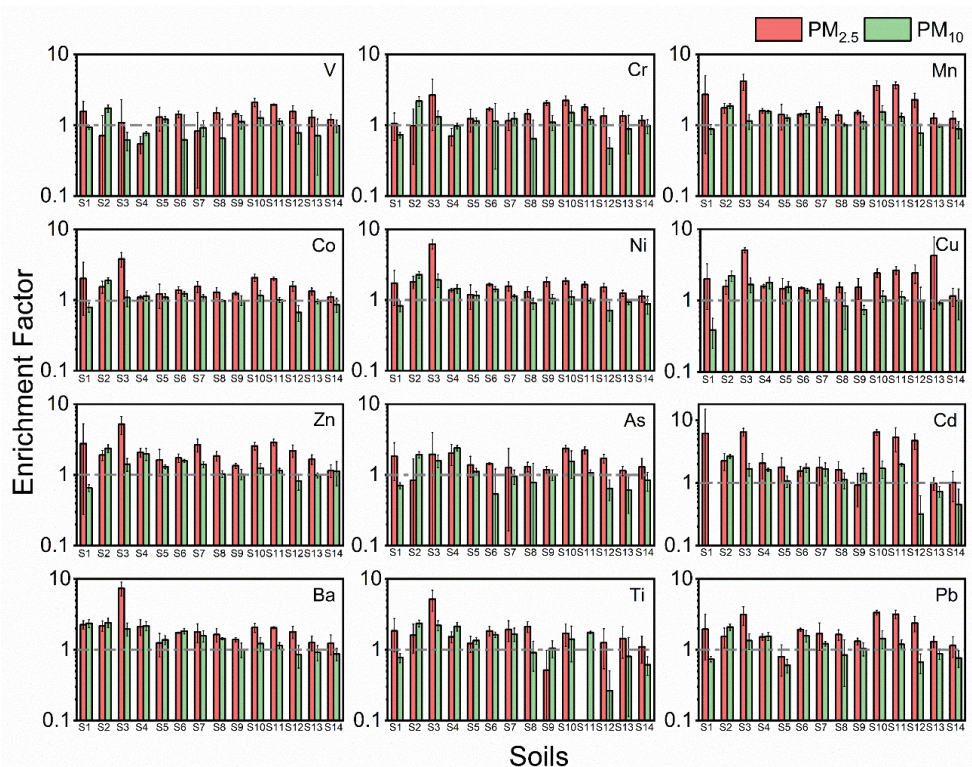
251 Where  $C_1$  is the heavy metal concentration in dust-PM;  $m_1$  is the mass of dust-PM collected on the  
252 filter;  $m_0$  is the mass of soil in the ICP-MS sample, and  $C_0$  is the heavy metal concentration of the  
253 soil.

254

255 [Figures 1](#) and [S7](#) show that many heavy metals were highly enriched in fine dust aerosols ( $PM_{2.5}$ ),  
256 i.e., their absolute concentrations were significantly higher in fine dust particles than in the parent  
257 soil ([Fig. S6](#)). V, Cr, Mn, Co, Ni, Cu, Zn, As, Cd, Ba, Ti, and Pb were all enriched in dust- $PM_{2.5}$   
258 during the process of dust formation. The following trend of heavy metal enrichment was  
259 established for dust- $PM_{2.5}$ :  $Cd > Zn > Ba > Cu > Mn > Pb > Ni > Ti > Co > As > Cr > V$ . Notably,  
260 the EFs of Cd were greater than 5 for soil S1, S10 and S11. [Fig. 1](#) also illustrates that all heavy  
261 metals were more highly enriched in smaller  $PM_{2.5}$  dust particles compared to larger  $PM_{10}$  dust  
262 particles. For example, the Cd's EF reached ~6.4 and ~1.7 for dust- $PM_{2.5}$  and dust  $PM_{10}$ , respectively,  
263 from soil S1. Most dust- $PM_{2.5}$  should originate from the small colloids in soil, which are defined as  
264 soil particles with less than 2  $\mu m$  in diameter. These soil colloids usually carry large amounts of  
265 negative charges, which can help adsorb many cations in soil, including various heavy metal ions  
266 ([Brady and Weil, 2008](#)). Thus, heavy metals are enriched in small soil aggregates. During the  
267 sandblasting process, the smaller soil grains, with higher heavy metal concentrations, are more  
268 likely to be ejected and form dust aerosols. The particle size dependence of heavy metal enrichment  
269 could have significant ramifications for the health impacts of dust aerosols. The dust aerosol size



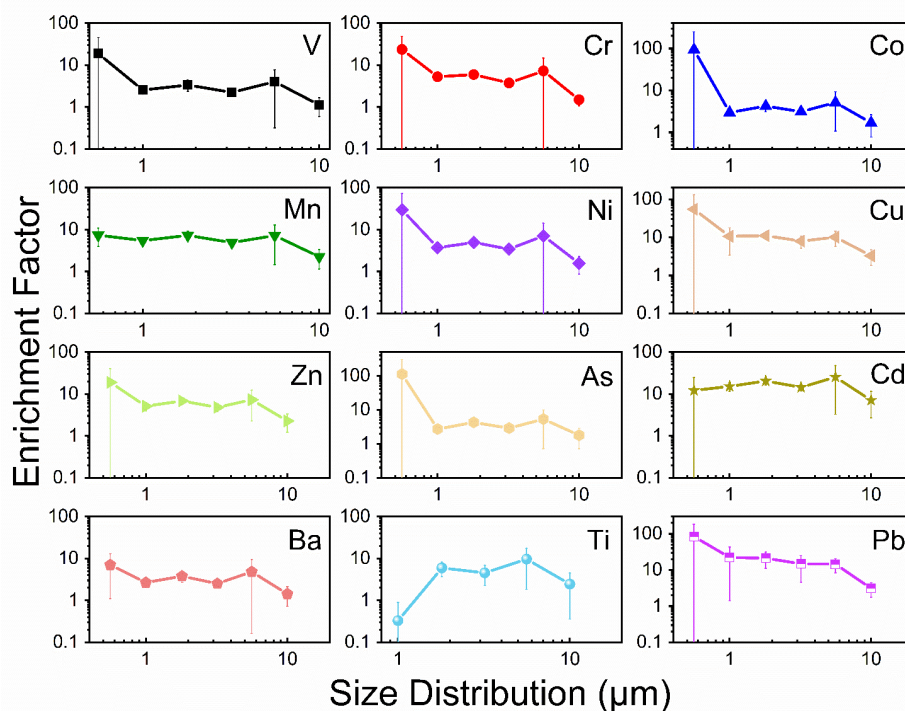
270 distribution of dust (Fig. S8) was also measured by an Aerodynamic Particle Sizer (APS,  
271 APS Model 3321; TSI Inc.; USA). It is found that the peak of the particle size distribution of dust  
272 was approximately at 2~3  $\mu\text{m}$ . Similarly, the scanning electron microscope (SEM) images of these  
273 dust aerosols (generated by S10) also show the presence of a large number of particles with sizes of  
274 2~3  $\mu\text{m}$ . As particle size decreased, the shape of particles changed from flakes to rods, which means  
275 a larger surface area (Fig. S9). As for the influence of soil texture on dust aerosol enrichment, we  
276 have not found any regularity and need to further explore.



277  
278 **Figure 1.** Enrichment Factors of  $\text{PM}_{2.5}$  and  $\text{PM}_{10}$ . Enrichment factors of heavy metals in dust  
279 aerosols from soil S1-S14; red represents  $\text{PM}_{2.5}$  and green represents  $\text{PM}_{10}$ . The grey dotted line  
280 represents the EF as 1. The whiskers on the bars represent the standard deviations of triplicates.  
281



282 To investigate the link between dust particle size and heavy metal EFs in greater detail, a MOUDI  
283 impactor was used to collect dust-PM from 0.56 to 10  $\mu\text{m}$  (absolute concentration obtained in Fig.  
284 S10). Consistent with the results discussed above, the EFs for some heavy metals, such as Pb,  
285 significantly increased with decreasing particle diameter ( $r = -1$ ,  $p < 0.01$ ) (Fig. 2). For the smallest  
286 dust particles (0.56–1.0  $\mu\text{m}$ ), the EFs for Pb was approximately 83, an order of magnitude greater  
287 than the EFs ( $\sim 3$ ) for the largest dust particles ( $>10 \mu\text{m}$ ). This result demonstrates that some heavy  
288 metals are indeed enriched in smaller soil particles, which could be aerosolized during the  
289 sandblasting process. The particle size dependence of heavy metal enrichment could have  
290 significant ramifications for the health impacts of dust aerosols.



291  
292 **Figure 2.** Enrichment factors of heavy metals in dust aerosols with different particle size ranges.  
293 The EF data were produced from the Soil S10, with diameters at above 10  $\mu\text{m}$ , 5.6–10  $\mu\text{m}$ , 3.2–5.6  
294  $\mu\text{m}$ , 1.8–3.2  $\mu\text{m}$ , 1.0–1.8  $\mu\text{m}$  and 0.56–1.0  $\mu\text{m}$ . The whiskers on the bars represent the standard



295 deviations of triplicates.

296

### 297 **3.2 Modeling of the contributions of dust aerosols to atmospheric heavy metals** 298 **using the dust profiles from this study and the SPECIATE datasets**

299 It is necessary to know the sources of atmospheric heavy metals to effectively control their emission.

300 Air quality models with emission inventories can estimate the contributions of various sources to

301 atmospheric heavy metals. However, when estimating heavy metal emissions from dust production,

302 some widely used air quality models, such as the CMAQ model, typically use dust profiles from the

303 US EPA's SPECIATE datasets. As discussed in the introduction, this dust profile may be outdated

304 and cannot reflect realistic dust compositions. We used the CMAQ model to assess the potential

305 impact of dust aerosol profile in atmospheric dust aerosol using our measured profile and the profile

306 (No. 41350) from the SPECIATE datasets. The model tracked heavy metals in PM<sub>2.5</sub> in China for

307 the year 2013 (see Methods) from five major sources: windblown dust, residential, transportation,

308 power generation, and industry.

309

310 [Figure 3](#) shows the modeled contributions of the dust source to the Cr and Pb concentrations in

311 PM<sub>2.5</sub> for China, using the measured soil, dust-PM<sub>2.5</sub> profiles from this study, as well as the

312 SPECIATE composition profiles (see Methods). In addition, the modeled results for other metals,

313 such as As, Cr, Mn, Ti, and Zn were presented in [Fig. S11-15](#).

314

315 For atmospheric Cr, it is clear that the scenario of applying SPECIATE database significantly

316 underestimates the contribution of dust aerosol, with the highest value of  $\sim 0.08 \mu\text{g}/\text{m}^3$ , when





317 compared to the scenario of applying the measured dust-PM<sub>2.5</sub> profiles, which had the highest value  
318 of  $\sim 0.14 \mu\text{g}/\text{m}^3$ . For Pb, as shown in the right column of Fig. 3, the scenario of applying  
319 SPECIATE profile overestimates the contribution of dust aerosol, with the value up to  $\sim 0.4 \mu\text{g}/\text{m}^3$ ,  
320 when compared to the scenario of applying the measured dust-PM<sub>2.5</sub> profiles, which had the highest  
321 value of  $\sim 0.14$ . These results demonstrate that the modeled heavy metal distribution in the  
322 atmosphere is quite sensitive to the input of dust composition profile, strongly suggesting that using  
323 a proper dust composition profile is a key in such air quality modeling.

324

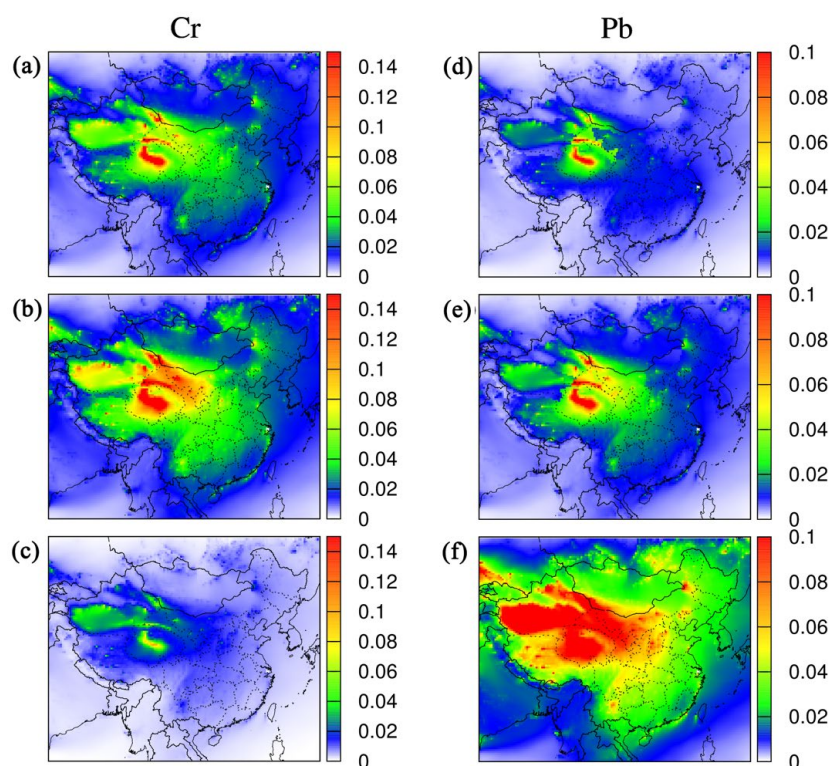
325 As discussed in the Introduction, many atmospheric studies assume that dust aerosol composition  
326 is similar to the composition of its parent soil. Here we also use the soil composition as an input  
327 dust profile in the model calculation to see how the modeled results are compared to that using the  
328 dust-PM<sub>2.5</sub> profile. For Cr, an obvious elevation of contribution was found by comparing the map  
329 using soil (a) and dust-PM<sub>2.5</sub> (b) profiles, with the hotspots of contribution ( $\sim 0.14 \mu\text{g}/\text{m}^3$ )  
330 distributed in northwest China. The region with dust aerosol contribution ranged from 0.02 to 0.08  
331  $\mu\text{g}/\text{m}^3$  covers most areas in China by using the dust-PM<sub>2.5</sub> profile. In contrast, the scenario of  
332 applying soil profile shows smaller areas. For Pb, a significant difference is also found. The high  
333 contribution areas are also mainly distributed in northwest China for scenarios of applying soil and  
334 dust profiles, with the value up to  $0.1 \mu\text{g}/\text{m}^3$ . While the area with low dust aerosol contribution  
335 ( $< 0.02 \mu\text{g}/\text{m}^3$ ) shrinks considerably in the scenario of applying soil profile.

336

337 The applied dust enrichment factors to modeled Cr in PM<sub>2.5</sub> had an even stronger impact on modeled  
338 source apportionment (Fig. 3a-3b). The average dust source contribution to the total PM<sub>2.5</sub> Cr



339 concentration over China was calculated to be 0.03, and 0.05  $\mu\text{g}/\text{m}^3$  in the scenarios of applying  
340 soil and dust profiles, respectively. The model results for As, Cu, Mn, Ti and Zn (Fig. S11-S15) also  
341 show similar trends, indicating applying realistic enrichment factors to heavy metal concentrations  
342 in fine dust aerosols is critical to accurately model the sources of atmospheric heavy metals. These  
343 results demonstrate that it is not appropriate to assume dust aerosol composition is equal to soil  
344 composition, at least in air quality modeling.

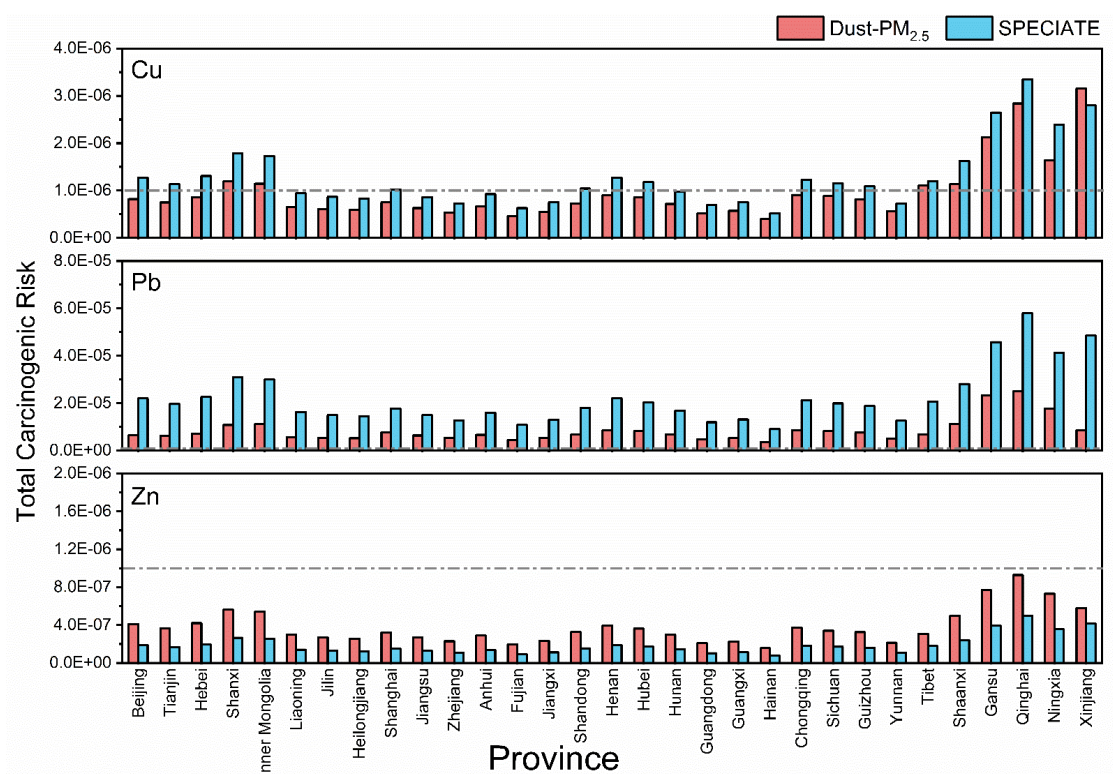


345  
346 **Figure 3.** Modeling of the contributions of dust aerosols to atmospheric Cr and Pb concentrations.  
347 These results use the dust profiles of measured soil (a, d), dust-PM<sub>2.5</sub> (b, e), and the SPECIATE  
348 datasets (c, f). The unit is  $\mu\text{g}/\text{m}^3$ .

349 Figure 4 shows the total carcinogenic risk (TCR) of the modeled atmospheric heavy metals (Cu, Pb  
350 and Zn) for each province in Mainland, China. The modeled results using the dust-PM<sub>2.5</sub> and the



351 SPECIATE profiles are compared here. The carcinogenic risks lower than  $10^{-6}$  are considered  
352 negligible, and risks above  $10^{-4}$  are not accepted by most international regulatory agencies (Cheng  
353 et al., 2015; Epa, 1989; Luo et al., 2012). For Cu, it is evident that using the SPECIATE profile  
354 overestimated (the difference range up to  $\sim 7.5 \times 10^{-7}$ ) the TCR in China compared to using the dust-  
355  $PM_{2.5}$  profile, as some regions exceed  $10^{-6}$ , the threshold value. For Pb, although all regions were  
356 above  $10^{-6}$ , the TCR using the SPECIATE profile was greatly overestimated (the difference range is  
357  $\sim 5.5 \times 10^{-6} - 4.0 \times 10^{-5}$ ). The model results for Zn showed that all regions were not above  $10^{-6}$  but  
358 significantly underestimated risks using the SPECIATE profile. This indicates that the health risk  
359 assessment is also sensitive to dust composition profiles. Using the SPECIATE profile might be  
360 problematic for assessing these risks.



361



362 **Figure 4.** Comparison of the total carcinogenic risk (TCR) of the modeled atmospheric heavy metals  
363 for each province in Mainland, China between using the dust-PM<sub>2.5</sub> and SPECIATE profiles. Here,  
364 the TCR of Cu, Pb and Zn were calculated. The grey dotted line is 10<sup>-6</sup>, the threshold value for  
365 health concerns.

366

### 367 **3.3 Field observation before, during and after a dust storm**

368 Our modeling results demonstrate that dust aerosol is the main source of multiple heavy metals in  
369 PM<sub>2.5</sub> in China. Therefore, dust storms should significantly increase the concentrations of heavy  
370 metals in PM<sub>2.5</sub>. To test this idea, we studied a dust-storm plume, which originated from Mongolia  
371 and arrived in Shanghai (Huang et al., 2010) on 23 May 2018 (Fig. S16). Real-time single-particle  
372 mass spectra were generated by a single-particle mass spectrometer. Single particle mass  
373 spectrometry can offer detailed information on the chemically-resolved mixing state at the single-  
374 particle level. According to the similarities of the mass-to-charge ratio and peak intensity of  
375 characterized signals, “Dust” particles were classified via an adaptive resonance theory-based  
376 clustering method (ART-2a, see Method). The number fraction of *Dust* particles was ~4.94% before  
377 and after the dust storm and it increased to ~9.73% during the dust storm episode (Fig. 5a).

378

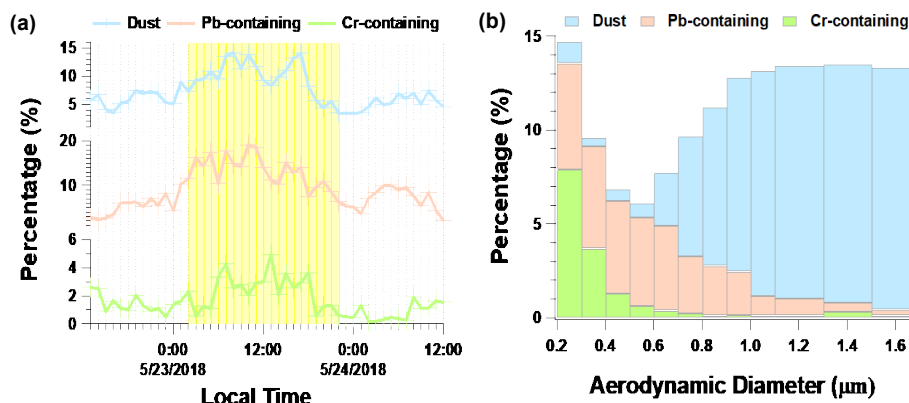
379 *Dust* particle mass spectra also contained ion markers indicative of an array of heavy metals (*m/z*  
380 55[Mn<sup>+</sup>], 51[V<sup>+</sup>], 207[Pb<sup>+</sup>], 63[Cu<sup>+</sup>], 75[As<sup>+</sup>], 91[AsO<sup>+</sup>], 52[Cr<sup>+</sup>], -84[CrO<sub>2</sub>], -100[CrO<sub>3</sub><sup>-</sup>]) (red  
381 sticks in Fig. S17), indicating the existence of heavy metals in the ambient dust aerosols. The time  
382 series of Pb-containing and Cr-containing particle number fractions showed similar trends to the  
383 *Dust* particles. When the dust storm arrived, both Pb-containing and Cr-containing particle fractions



384 increased as the dust cluster fraction increased. Before and after the dust storm, the percentages of  
385 Pb-containing and Cr-containing particles that overlapped with the *Dust* cluster were 41% and 32%,  
386 respectively. However, this overlapped ratio increased to 86% and 71% during the dust storm  
387 episode. The increase of heavy metal particles in step with the dust particles indicated the dust  
388 particles could be the dominant source of these heavy metal species during this dust storm episode.

389

390 We further analyzed the size-resolved number fraction of dust aerosol, Pb-containing, and Cr-  
391 containing particles during the dust storm episode (Fig. 5b). The number fraction of *Dust* particles  
392 increased with increasing aerodynamic diameter. For particles above 1.0  $\mu\text{m}$ , *Dust* accounted  
393 for >12% of the total particles during the storm. However, the Pb-containing and Cr-containing  
394 particles made up a larger number fraction of analyzed particles with decreasing particle diameter  
395 size (< 1  $\mu\text{m}$ ). The number fractions of Pb-containing and Cr-containing particles were 5.7% and  
396 7.9% of all mass spectra for particles from 0.2-0.3  $\mu\text{m}$ . This result was consistent with our laboratory  
397 results that there is high heavy metal enrichment in smaller dust particles and our modeling results  
398 that dust aerosol is likely a major source of atmospheric Pb and Cr over China.



399  
400 **Figure 5.** Ambient dust aerosol measurements. (a) Temporal variation of the percentages of dust  
401 aerosol, Pb-containing, and Cr-containing particle clusters. The yellow shadow represents the dust  
402 storm episode. (b) Size-resolved number fraction of dust aerosol, Pb-containing, and Cr-containing  
403 particle clusters.  
404

#### 405 **4 Environmental implications**

406 In this study, many heavy metals were found to be highly enriched in fine ( $PM_{2.5}$ ) dust aerosols  
407 compared to their concentrations in the parent soils. We propose that heavy metals tend to be  
408 enriched in smaller soil aggregates (Ikegami et al., 2014). During the sandblasting process, the  
409 heavy metal enriched smaller soil aggregates are more likely to be ejected and form dust aerosols.  
410 This work finds that dust aerosols from different soils may have a range of heavy metal enrichment  
411 factors. To study the transfer of heavy metals from soils to the air, it is critical to have a complete  
412 set of enrichment factors for each major soil type. There exists a difference among the heavy metal  
413 enrichment factors from different soil samples. The variability in the EFs is likely due to differences  
414 in soil properties (soil texture and size distribution etc.) which may affect the sandblasting/saltation



415 process. For example, the enrichment factors of heaviest metals for Soil S1, S10 and S11 were  
416 higher than other soils. The detailed reason is still unknown and needs further exploration. Moreover,  
417 air quality models, including CMAQ models and various CMB models, often use the dust chemical  
418 profiles from the US EPA's SPECIATE to calculate the contribution of fine dust aerosols to  
419 atmospheric heavy metals, which are outdated and could lead to significant errors in estimating the  
420 emission of heavy metals through dust generation. Without using proper dust profiles in estimating  
421 heavy metal emissions from dust generation, the contribution of fine dust aerosols to atmospheric  
422 heavy metals, and its associated health risks are likely significantly mistaken.

## 423 **5. Conclusions**

424 Dust generation and aerosolization are complex processes that may have certain chemical selectivity.  
425 Here, we deployed a laboratory generator to produce dust aerosol with a realistic sandblasting  
426 process. The concentrations of heavy metals (including V, Cr, Mn, Co, Ni, Cu, Zn, As, Cd, Ba,  
427 Ti, and Pb) in soils and fine ( $PM_{2.5}$ ) and coarse ( $PM_{10}$ ) dust aerosols were measured. With  
428 research efforts to elucidate the enrichment process of heavy metal in dust aerosols comparing  
429 to their parent soils, our results fill the knowledge gaps of the compositional variation of heavy  
430 metal between the parent soils and the generated dust aerosols. Mn, Cd, Pb and other heavy  
431 metals were found to be highly enriched in fine ( $PM_{2.5}$ ) dust aerosols, which can be up to ~6.5-  
432 fold. These findings were also consistent with our field observation results. In addition, air  
433 quality models often use an outdated heavy metal profile for dust aerosols from the US EPA's  
434 SPECIATE database, which seems to be lack of enrichment between each particle size. We modeled  
435 the impact of the contribution of heavy metals in dust aerosol and their health risks in CMAQ,



436 a widely used air quality model, and determined that atmospheric heavy metal concentrations  
437 over China, which drastically changed when we applied different dust profiles, such as the  
438 measured soil, dust-PM<sub>2.5</sub> profiles from this study, as well as the SPECIATE composition  
439 profiles. Our air quality modeling for China demonstrates that the calculated contribution of fine  
440 dust aerosols to atmospheric heavy metals, as well as their cancer risks, could have significant errors  
441 without using proper dust profiles.

#### 442 **Supplement**

443 The supplement related to this article is available online at: <http://dx.doi.org/0.17632/byg6xk2fe9.1>.

#### 444 **Data availability**

445 All data supporting this study and its findings will be available in an online data repository at:  
446 <http://dx.doi.org/10.17632/wpphf8rd33.1>.

#### 447 **Author contributions**

448 X.W. and J.C. conceptualized the work and designed the experiments. H.Z. and S.Z. led the air  
449 quality modeling work. Q.G. lead the experimental work of heavy metal enrichment measurements.  
450 J.Z. led the field observation. K.Z., Q.W., S.C., S.W., J.H., X.L. and H.C. helped in experimental  
451 works. L.Z., L.W., Z.W., X.Y. and H.Z. helped in the experimental design and data analysis. Q.Y.  
452 provided the data required for the air quality modeling. All authors contributed to the paper's writing.  
453





454 **Competing interests**

455 The authors declare no competing interests.

456 **Disclaimer**

457 Publisher's note: Copernicus Publications remains neutral with regard to jurisdictional claims in  
458 published maps and institutional affiliations.

459

460 **Acknowledgements**

461 The authors also thank Xingxing Wang and Xiangcheng Zeng for their help in heavy metal measurement.

462 **Financial support**

463 This work was partially supported by the National Natural Science Foundation of China (Nos.  
464 92044301, 42077193, 21906024). Comments from Dr. Camille Sultana greatly improved this  
465 manuscript.

466 **Reference**

467 Alfaro, S. C.: Influence of soil texture on the binding energies of fine mineral dust particles  
468 potentially released by wind erosion, *Geomorphology*, 93, 157-167,  
469 10.1016/j.geomorph.2007.02.012, 2008.  
470 Ashrafi, K., Fallah, R., Hadei, M., Yarahmadi, M., and Shahsavani, A.: Source apportionment of  
471 total suspended particles (TSP) by positive matrix factorization (PMF) and chemical mass balance  
472 (CMB) modeling in Ahvaz, Iran, *Archives of environmental contamination and toxicology*, 75, 278-  
473 294, 2018.



- 474 Balakrishna, G. and Pervez, S.: Source apportionment of atmospheric dust fallout in an urban-  
475 industrial environment in India, *Aerosol and Air Quality Research*, 9, 359-367, 2009.
- 476 Becagli, S., Caiazzo, L., Di Iorio, T., di Sarra, A., Meloni, D., Muscari, G., Pace, G., Severi, M., and  
477 Traversi, R.: New insights on metals in the Arctic aerosol in a climate changing world, *Science of  
478 The Total Environment*, 741, 140511, <https://doi.org/10.1016/j.scitotenv.2020.140511>, 2020.
- 479 Brady, N. and Weil, R.: *The nature and properties of soils*, Pearson Education, Inc.0135133874,  
480 2008.
- 481 Bryant, R. G.: Recent advances in our understanding of dust source emission processes, *Progress in  
482 Physical Geography-Earth and Environment*, 37, 397-421, 10.1177/0309133313479391, 2013.
- 483 Burezq, H.: Combating wind erosion through soil stabilization under simulated wind flow condition  
484 - Case of Kuwait, *International Soil and Water Conservation Research*, 8, 154-163,  
485 10.1016/j.iswcr.2020.03.001, 2020.
- 486 Chang, A. C., Warneke, J. E., Page, A. L., and Lund, L. J.: Accumulation of Heavy Metals in Sewage  
487 Sludge-Treated Soils, *Journal of Environmental Quality*, 13, 87-91,  
488 <https://doi.org/10.2134/jeq1984.00472425001300010016x>, 1984.
- 489 Cheng, I., Xu, X., and Zhang, L.: Overview of receptor-based source apportionment studies for  
490 speciated atmospheric mercury, *Atmospheric Chemistry and Physics*, 15, 7877-7895, 10.5194/acp-  
491 15-7877-2015, 2015.
- 492 Ding, R. Q., Li, J. P., Wang, S. G., and Ren, F. M.: Decadal change of the spring dust storm in  
493 northwest China and the associated atmospheric circulation, *Geophysical Research Letters*, 32,  
494 10.1029/2004gl021561, 2005.
- 495 EPA, A.: Risk assessment guidance for superfund. Volume I: human health evaluation manual (part  
496 a), EPA/540/1-89/002, 1989.
- 497 Evan, A. T., Flamant, C., Fiedler, S., and Doherty, O.: An analysis of aeolian dust in climate models,  
498 *Geophysical Research Letters*, 41, 5996-6001, 10.1002/2014gl060545, 2014.
- 499 Gholizadeh, A., Taghavi, M., Moslem, A., Neshat, A. A., Najafi, M. L., Alahabadi, A., Ahmadi, E.,  
500 Asour, A. A., Rezaei, H., and Gholami, S.: Ecological and health risk assessment of exposure to  
501 atmospheric heavy metals, *Ecotoxicology and environmental safety*, 184, 109622, 2019.
- 502 Gillette, D. and Goodwin, P. A.: Microscale transport of sand-sized soil aggregates eroded by wind,  
503 *Journal of Geophysical Research*, 79, 4080-4084, 10.1029/JC079i027p04080, 1974.
- 504 Griggs, D. J. and Noguer, M.: *Climate change 2001: the scientific basis. Contribution of working  
505 group I to the third assessment report of the intergovernmental panel on climate change*, *Weather*,  
506 57, 267-269, 2002.
- 507 Grini, A. and Zender, C. S.: Roles of saltation, sandblasting, and wind speed variability on mineral  
508 dust aerosol size distribution during the Puerto Rican Dust Experiment (PRIDE), *Journal of  
509 Geophysical Research-Atmospheres*, 109, 10.1029/2003jd004233, 2004.
- 510 Grini, A., Zender, C. S., and Colarco, P. R.: Saltation Sandblasting behavior during mineral dust  
511 aerosol production, *Geophysical Research Letters*, 29, 10.1029/2002gl015248, 2002.
- 512 Guenther, A. B., Jiang, X., Heald, C. L., Sakulyanontvittaya, T., Duhl, T., Emmons, L. K., and Wang,  
513 X.: The Model of Emissions of Gases and Aerosols from Nature version 2.1 (MEGAN2.1): an  
514 extended and updated framework for modeling biogenic emissions, *Geoscientific Model  
515 Development*, 5, 1471-1492, 10.5194/gmd-5-1471-2012, 2012.
- 516 Gunawardana, C., Goonetilleke, A., Egodawatta, P., Dawes, L., and Kokot, S.: Source  
517 characterisation of road dust based on chemical and mineralogical composition, *Chemosphere*, 87,



- 518 163-170, 10.1016/j.chemosphere.2011.12.012, 2012.
- 519 Huang, K., Zhuang, G. S., Li, J. A., Wang, Q. Z., Sun, Y. L., Lin, Y. F., and Fu, J. S.: Mixing of  
520 Asian dust with pollution aerosol and the transformation of aerosol components during the dust  
521 storm over China in spring 2007, *Journal of Geophysical Research-Atmospheres*, 115,  
522 10.1029/2009jd013145, 2010.
- 523 Huebert, B. J., Bates, T., Russell, P. B., Shi, G. Y., Kim, Y. J., Kawamura, K., Carmichael, G., and  
524 Nakajima, T.: An overview of ACE-Asia: Strategies for quantifying the relationships between Asian  
525 aerosols and their climatic impacts, *Journal of Geophysical Research-Atmospheres*, 108,  
526 10.1029/2003jd003550, 2003.
- 527 Huneus, N., Schulz, M., Balkanski, Y., Griesfeller, J., Prospero, J., Kinne, S., Bauer, S., Boucher,  
528 O., Chin, M., Dentener, F., Diehl, T., Easter, R., Fillmore, D., Ghan, S., Ginoux, P., Grini, A.,  
529 Horowitz, L., Koch, D., Krol, M. C., Landing, W., Liu, X., Mahowald, N., Miller, R., Morcrette, J.  
530 J., Myhre, G., Penner, J., Perlwitz, J., Stier, P., Takemura, T., and Zender, C. S.: Global dust model  
531 intercomparison in AeroCom phase I, *Atmospheric Chemistry and Physics*, 11, 7781-7816,  
532 10.5194/acp-11-7781-2011, 2011.
- 533 Ikegami, M., Yoneda, M., Tsuji, T., Bannai, O., and Morisawa, S.: Effect of Particle Size on Risk  
534 Assessment of Direct Soil Ingestion and Metals Adhered to Children's Hands at Playgrounds, *Risk  
535 Analysis*, 34, 1677-1687, 10.1111/risa.12215, 2014.
- 536 Kaufman, Y. J., Tanre, D., and Boucher, O.: A satellite view of aerosols in the climate system, *Nature*,  
537 419, 215-223, 10.1038/nature01091, 2002.
- 538 Kok, J. F., Ward, D. S., Mahowald, N. M., and Evan, A. T.: Global and regional importance of the  
539 direct dust-climate feedback, *Nature Communications*, 9, 10.1038/s41467-017-02620-y, 2018.
- 540 Kok, J. F., Storelvmo, T., Karydis, V. A., Adebisi, A. A., Mahowald, N. M., Evan, A. T., He, C., and  
541 Leung, D. M.: Mineral dust aerosol impacts on global climate and climate change, *Nature Reviews  
542 Earth & Environment*, 10.1038/s43017-022-00379-5, 2023.
- 543 Lafon, S., Alfaro, S. C., Chevaillier, S., and Rajot, J. L.: A new generator for mineral dust aerosol  
544 production from soil samples in the laboratory: GAMEL, *Aeolian Research*, 15, 319-334,  
545 <https://doi.org/10.1016/j.aeolia.2014.04.004>, 2014.
- 546 Li, L., Huang, Z. X., Dong, J. G., Li, M., Gao, W., Nian, H. Q., Fu, Z., Zhang, G. H., Bi, X. H.,  
547 Cheng, P., and Zhou, Z.: Real time bipolar time-of-flight mass spectrometer for analyzing single  
548 aerosol particles, *International Journal of Mass Spectrometry*, 303, 118-124,  
549 10.1016/j.ijms.2011.01.017, 2011.
- 550 Liu, X. D., Yin, Z. Y., Zhang, X. Y., and Yang, X. C.: Analyses of the spring dust storm frequency  
551 of northern China in relation to antecedent and concurrent wind, precipitation, vegetation, and soil  
552 moisture conditions, *Journal of Geophysical Research-Atmospheres*, 109, 10.1029/2004jd004615,  
553 2004.
- 554 Lowenthal, D. H., Watson, J. G., Koracin, D., Chen, L.-W. A., Dubois, D., Vellore, R., Kumar, N.,  
555 Knipping, E. M., Wheeler, N., and Craig, K.: Evaluation of regional-scale receptor modeling,  
556 *Journal of the Air & Waste Management Association*, 60, 26-42, 2010.
- 557 Luo, X.-S., Ding, J., Xu, B., Wang, Y.-J., Li, H.-B., and Yu, S.: Incorporating bioaccessibility into  
558 human health risk assessments of heavy metals in urban park soils, *Science of the Total Environment*,  
559 424, 88-96, 2012.
- 560 Lv, M., Hu, A., Chen, J., and Wan, B.: Evolution, Transport Characteristics, and Potential Source  
561 Regions of PM<sub>2.5</sub> and O<sub>3</sub> Pollution in a Coastal City of China during 2015–2020, *Atmosphere*, 12,



- 562 1282, 2021.
- 563 Middleton, N., Tozer, P., and Tozer, B.: Sand and dust storms: underrated natural hazards, *Disasters*,  
564 43, 390-409, 10.1111/disa.12320, 2019.
- 565 Miller, M. S., Friedlander, S. K., and Hidy, G. M.: A chemical element balance for the Pasadena  
566 aerosol, *Journal of Colloid and Interface Science*, 39, 165-176, [https://doi.org/10.1016/0021-](https://doi.org/10.1016/0021-9797(72)90152-X)  
567 9797(72)90152-X, 1972.
- 568 Naderizadeh, Z., Khademi, H., and Ayoubi, S.: Biomonitoring of atmospheric heavy metals  
569 pollution using dust deposited on date palm leaves in southwestern Iran, *Atmósfera*, 29, 141-155,  
570 10.20937/ATM.2016.29.02.04, 2016.
- 571 Parajuli, S. P., Zobeck, T. M., Kocurek, G., Yang, Z. L., and Stenchikov, G. L.: New insights into  
572 the wind-dust relationship in sandblasting and direct aerodynamic entrainment from wind tunnel  
573 experiments, *Journal of Geophysical Research-Atmospheres*, 121, 1776-1792,  
574 10.1002/2015jd024424, 2016.
- 575 Perlwitz, J. P., Pérez García-Pando, C., and Miller, R. L.: Predicting the mineral composition of dust  
576 aerosols – Part 1: Representing key processes, *Atmos. Chem. Phys.*, 15, 11593-11627, 10.5194/acp-  
577 15-11593-2015, 2015.
- 578 Pongkiatkul, P. and Kim Oanh, N. T.: Assessment of potential long-range transport of particulate air  
579 pollution using trajectory modeling and monitoring data, *Atmospheric Research*, 85, 3-17,  
580 <https://doi.org/10.1016/j.atmosres.2006.10.003>, 2007.
- 581 Prospero, J. M., Ginoux, P., Torres, O., Nicholson, S. E., and Gill, T. E.: Environmental  
582 characterization of global sources of atmospheric soil dust identified with the Nimbus 7 Total Ozone  
583 Mapping Spectrometer (TOMS) absorbing aerosol product, *Reviews of geophysics*, 40, 2-1-2-31,  
584 2002.
- 585 Samiksha, S., Raman, R. S., Nirmalkar, J., Kumar, S., and Sirvaiya, R.: PM10 and PM2.5 chemical  
586 source profiles with optical attenuation and health risk indicators of paved and unpaved road dust  
587 in Bhopal, India, *Environmental Pollution*, 222, 477-485, 2017.
- 588 Santos, J. M., Reis, N. C., Galvão, E. S., Silveira, A., Goulart, E. V., and Lima, A. T.: Source  
589 apportionment of settleable particles in an impacted urban and industrialized region in Brazil,  
590 *Environmental Science and Pollution Research*, 24, 22026-22039, 2017.
- 591 Shangguan, Y., Zhuang, X., Querol, X., Li, B., Moreno, N., Trechera, P., Sola, P. C., Uzu, G., and  
592 Li, J.: Characterization of deposited dust and its respirable fractions in underground coal mines:  
593 Implications for oxidative potential-driving species and source apportionment, *International Journal*  
594 *of Coal Geology*, 258, 104017, <https://doi.org/10.1016/j.coal.2022.104017>, 2022.
- 595 Shao, Y. and Dong, C. H.: A review on East Asian dust storm climate, modelling and monitoring,  
596 *Global and Planetary Change*, 52, 1-22, 10.1016/j.gloplacha.2006.02.011, 2006.
- 597 Shao, Y. and Raupach, M. R.: Effect of saltation bombardment on the environment of dust by wind,  
598 *Journal of Geophysical Research-Atmospheres*, 98, 12719-12726, 10.1029/93jd00396, 1993.
- 599 Shao, Y. P., Klose, M., and Wyrwoll, K. H.: Recent global dust trend and connections to climate  
600 forcing, *Journal of Geophysical Research-Atmospheres*, 118, 11107-11118, 10.1002/jgrd.50836,  
601 2013.
- 602 Shao, Y. P., Raupach, M. R., and Leys, J. F.: A model for predicting aeolian sand drift and dust  
603 entrainment on scales from paddock to region, *Australian Journal of Soil Research*, 34, 309-342,  
604 10.1071/sr9960309, 1996.
- 605 Simon, H., Beck, L., Bhave, P. V., Divita, F., Hsu, Y., Luecken, D., Mobley, J. D., Pouliot, G. A.,



- 606 Reff, A., and Sarwar, G.: The development and uses of EPA's SPECIATE database, *Atmospheric*  
607 *Pollution Research*, 1, 196-206, 2010.
- 608 Sullivan, R., Guazzotti, S., Sodeman, D., and Prather, K.: Direct observations of the atmospheric  
609 processing of Asian mineral dust, *Atmospheric Chemistry and Physics*, 7, 1213-1236, 2007.
- 610 Tang, M. J., Cziczo, D. J., and Grassian, V. H.: Interactions of Water with Mineral Dust Aerosol:  
611 Water Adsorption, Hygroscopicity, Cloud Condensation, and Ice Nucleation, *Chemical Reviews*,  
612 116, 4205-4259, 10.1021/acs.chemrev.5b00529, 2016.
- 613 Textor, C., Schulz, M., Guibert, S., Kinne, S., Balkanski, Y., Bauer, S., Berntsen, T., Berglen, T.,  
614 Boucher, O., Chin, M., Dentener, F., Diehl, T., Easter, R., Feichter, H., Fillmore, D., Ghan, S.,  
615 Ginoux, P., Gong, S., Kristjansson, J. E., Krol, M., Lauer, A., Lamarque, J. F., Liu, X., Montanaro,  
616 V., Myhre, G., Penner, J., Pitari, G., Reddy, S., Seland, O., Stier, P., Takemura, T., and Tie, X.:  
617 Analysis and quantification of the diversities of aerosol life cycles within AeroCom, *Atmospheric*  
618 *Chemistry and Physics*, 6, 1777-1813, 10.5194/acp-6-1777-2006, 2006.
- 619 Urrutia-Pereira, M., Rizzo, L. V., Staffeld, P. L., Chong-Neto, H. J., Viegi, G., and Sole, D.: Dust  
620 from the Sahara to the American Continent: Health impacts, *Allergologia Et Immunopathologia*, 49,  
621 187-194, 10.15586/aei.v49i4.436, 2021.
- 622 Wu, F., Cheng, Y., Hu, T., Song, N., Zhang, F., Shi, Z., Hang Ho, S. S., Cao, J., and Zhang, D.:  
623 Saltation–Sandblasting Processes Driving Enrichment of Water-Soluble Salts in Mineral Dust,  
624 *Environmental Science & Technology Letters*, 2022.
- 625 Yang, Y. Q., Hou, Q., Zhou, C. H., Liu, H. L., Wang, Y. Q., and Niu, T.: Sand/dust storm processes  
626 in Northeast Asia and associated large-scale circulations, *Atmospheric Chemistry and Physics*, 8,  
627 25-33, 10.5194/acp-8-25-2008, 2008.
- 628 Ying, Q., Feng, M., Song, D., Wu, L., Hu, J., Zhang, H., Kleeman, M. J., and Li, X.: Improve  
629 regional distribution and source apportionment of PM<sub>2.5</sub> trace elements in China using inventory-  
630 observation constrained emission factors, *Science of the total environment*, 624, 355-365, 2018.
- 631 Zhang, H. R. and Tripathi, N. K.: Geospatial hot spot analysis of lung cancer patients correlated to  
632 fine particulate matter (PM<sub>2.5</sub>) and industrial wind in Eastern Thailand, *Journal of Cleaner*  
633 *Production*, 170, 407-424, 10.1016/j.jclepro.2017.09.185, 2018.
- 634 Zhuang, G. S., Guo, J. H., Yuan, H., and Zhao, C. Y.: The compositions, sources, and size  
635 distribution of the dust storm from China in spring of 2000 and its impact on the global environment,  
636 *Chinese Science Bulletin*, 46, 895-901, 10.1007/bf02900460, 2001.